Surface enhancement of molecular ion H_2^+ yield in a 2.45-GHz electron–cyclotron resonance ion source*

Yuan Xu(徐源)[1], Shi-Xiang Peng(彭士香)[1,†], Hai-Tao Ren(任海涛)[1], Ai-Lin Zhang(张艾霖)[1,2], Tao Zhang(张滔)[1], Jing-Feng Zhang(张景丰)[1], Jia-Mei Wen(温佳美)[1], Wen-Bin Wu(武文斌)[1], Zhi-Yu Guo(郭之虞)[1], and Jia-Er Chen(陈佳洱)[1,2]

[1] *State Key Laboratory of Nuclear Physics and Technology & Institute of Heavy Ion Physics, Peking University, Beijing* 100871, *China*
[2] *University of Chinese Academy of Sciences, Beijing* 100049, *China*

(Received 28 February 2017; revised manuscript received 2 May 2017; published online 20 June 2017)

High current hydrogen molecular ion beam is obtained with a specially designed stainless steel liner permanent magnet 2.45-GHz electron–cyclotron resonance (ECR) ion source (PMECR II) at Peking University (PKU). To further understand the physics of the hydrogen generation process inside a plasma chamber, theoretical and experimental investigations on the liner material of the plasma chamber in different running conditions are carried out. Several kinds of materials, stainless steel (SS), tantalum (Ta), quartz, and aluminum (Al) are selected in our study. Experimental results show that stainless steel and tantalum are much better than others in H_2^+ generation. During the experiment, an increasing trend in H_2^+ fraction is observed with stainless steel liner after O_2 discharge inside the ion source. Surface analyses show that the roughness change on the surface after O_2 discharge may be responsible for this phenomenon. After these studies, the pure current of H_2^+ ions can reach 42.3 mA with a fraction of 52.9%. More details are presented in this paper.

Keywords: H_2^+ ion source, ECR, 40 mA, plasma

PACS: 52.50.Dg, 52.50.Sw, 52.40.Hf, 52.59.–f **DOI:** 10.1088/1674-1056/26/8/085203

1. Introduction

The interest in high intensity H_2^+ ion source is increasing rapidly with the development of the worldwide high intensity proton cyclotron and D^+ linac. For instance, it is an effective way to accelerate H_2^+ in place of H^+ in high current cyclotrons to reduce the space charge effect during beam transportation.[1] Moreover, deuteron accelerators are widely used in neutron source such as Sprial 2,[2] Soreq applied research accelerator facility (SARAF),[3] etc. As neutron radiation is induced by D(d, n) reaction along the beam line,[4] it is proposed to use H_2^+ as a pilot beam in place of D^+ to be accelerated during the commissioning phase in order to reduce the radiation problem and to guarantee the safety of the facility and staff.

At Peking University (PKU), all permanent magnet 2.45-GHz ECR ion sources for singly charged and lowly charged ion generation have been developed in the past decades.[5,6] Recently, 40-mA H_2^+ and 20-mA H_3^+ ion beams were successfully generated by PMECR II — an SS ECR ion source in the plasma chambers with different diameters. Experimental results show that a plasma chamber with a diameter of 64 mm (no liner) and another one with a diameter of 30 mm (stainless steel (SS) liner) seem to be advantageous for molecular ions generation over those with other dimensions.[7]

Recently, special attention was paid to the physics of hydrogen generation processes within a plasma chamber with different liner materials. Waldmann and Ludewigt mounted different liners on the front and end plates of the plasma chamber in a 2.45-GHz microwave ion source.[8] It indicated that with BN or Al_2O_3, a higher proton fraction could be achieved. But with SS, the ratio of protons was relatively low. Jung *et al.* also investigated the suitable material of the plasma electrode for proton generation in a helicon ion source, and alumina that had a very low recombination possibility was concluded to be very effective.[9] However, there is no particular investigation concerning the dependence of hydrogen molecular ion on the plasma chamber surface. Here, SS, Ta, quartz, and Al are selected in our study. Experiments indicate that SS and Ta are much more suitable for the generation of H_2^+than others. A 42.3-mA H_2^+ ion beam is obtained with a fraction of 52.9%.

An obvious enhancement of H_2^+ fraction is witnessed after the SS plasma chamber operating with oxygen discharge for several hours during our experiments. This may indicate something changed on the SS surface after O_2 discharge. Possibly, except for the category of materials, the surface morphology also has an influence on the generation of molecular ions. Comparison experiment between a native SS surface and as SS surface after O_2 discharge are also carried out.

The rest of this paper is organized as follows. In Sec-

*Project supported by the National Natural Science Foundation of China (Grant Nos. 11175009 and 11575013).
†Corresponding author. E-mail: sxpeng@pku.edu.cn
© 2017 Chinese Physical Society and IOP Publishing Ltd

tion 2, some physical analyses of hydrogen plasma recombination processes are given. In Section 3, the function of material on the H_2^+ generation is displayed, showing the O_2influence on the ion fractions. Moreover, SS samples are placed on the chamber surface to simulate the bombardments of O^+ and H^+ on the wall. The analysis results of atomic force microscopy (AFM) and x-ray photoelectron spectroscopy (XPS) of the chamber surface are presented. More details are reported in this paper.

2. Physical analysis of recombination processes

In hydrogen plasmas, H_2^+ ions are produced inevitably by direct ionization of hydrogen molecular H_2:

$$e + H_2 \rightarrow H_2^+ + 2e.$$

Simultaneously, a proton is generated mainly by a two-step process as the electron temperature in 2.45-GHz ECR ion source at PKU is normally lower than 15 eV:[10]

$$e + H_2 \rightarrow 2H, H + e \rightarrow H^+.$$

If the number of H atoms in the plasma increases, it will be advantageous for proton, *vice versa*. So for an H_2^+ ion source, one should reduce the concentration of hydrogen atoms to some extent.

In addition, in ion sources, the recombination of hydrogen atoms tends to happen on the surface of the chamber wall:

$$H + H + \text{wall} \rightarrow H_2.^{[11]}$$

This recombination process will make the number of H atoms somehow decrease in the discharge volume. Practically, the possibility of recombination on the wall is determined mainly by the category of material, its morphology and temperature.[11] This leads to a big difference in recombination coefficient (γ) among numerous materials as shown in Table 1.[11] It can be seen that metals such as stainless steel, tantalum (Ta) have a relative high recombination coefficient with a magnitude of 10^{-1}; but for dielectric materials like quartz and oxide, their recombination coefficients are only around 10^{-3} $\sim 10^{-4}$ in magnitude. Obviously, for H_2^+ yield, a higher recombination possibility is preferred to reduce the number of H atoms.

Table 1. Atomic hydrogen recombination coefficients for various materials.[11,12]

Material	γ
Pure SS	0.1
Pure Ta	~ 0.1
Pure Al	~ 0.1
Quartz	$7.5\times10^{-4}\pm 0.8\times10^{-4}$
Native oxide-covered SS	$2.2\times10^{-3}\pm 0.2\times10^{-3}$
Native oxide-covered Al	$1.7\times10^{-3}\pm 0.2\times10^{-3}$

The surface morphology will also have a great influence on the recombination possibility. So, even with identical material, the recombination coefficient will change accompanied with varying of the surface morphology.

3. Experiments and discussion

The experimental ion source (PMECR II) and test bench were already described in detail in Ref. [13]. Briefly, the ion source was a 2.45-GHz permanent magnet ECR ion source. The magnetic field of the ion source was generated by three NdFeB rings. Then, a mixed beam with H^+, H_2^+, and H_3^+ was extracted through a three-electrode system with a Φ6-mm hole. The operation pressure was measured through the vacuum chamber connected to the extraction system. The total current was measured by a water-cooled Faraday cup, and the fraction of each species was analyzed by a 90° dipole magnet afterwards. The inner diameter of the experimental source was 64 mm, and the original chamber material of this source was SS. Generally, the material of the chamber surface was varied by inserting a cylindrical tube liner as shown in Fig. 1.

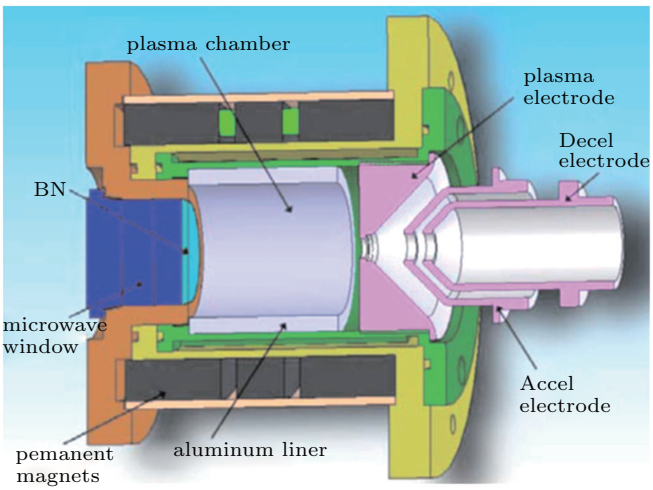


Fig. 1. (color online) Schematic diagram of ECR ion source at PKU.[5]

3.1. Investigations of liner material

Experiments were carried out under pulsed mode with a duty factor of 10% (100 Hz/1 ms). The extraction voltage in our experiment was fixed at 45 kV. Tube liners made of pure SS, pure Ta, pure Al, and quartz with the same dimension were used to change the surface of the plasma chamber. In Fig. 2, the pure current of H_2^+ varying with rf power is compared by putting different liner cylinders inside the ion source with other operation parameters remaining the same.

It is obvious in Fig. 2 that SS and Ta materials seem to have high potentials for producing more H_2^+ compared with quartz and Al. This may indicate that a high recombination coefficient material is advantageous for producing H_2^+.

Actually, the optimized operation parameters for H_2^+ production were always different with different materials. So, the maximum currents of H_2^+ that can be obtained with different materials are illustrated in Fig. 3. For SS and Ta, nearly 40-mA pure H_2^+ beam was extracted from the ion source. For quartz, whose γ is 7.5×10^{-4}, a lower H_2^+ production was shown. But for the Al liner, which actually should have very high recombination possibility, only 20-mA H_2^+ could be generated here. This was because a stable alumina layer could exist on the outer surface of metal Al even under hydrogen plasma bombardments which meant that the recombination coefficient of Al liner was actually very low compared with pure metal as shown in Table 1.[12] Furthermore, alumina also had a high secondary electron emission ability which was advantageous for the dissociation of H_2^+ and formation of proton.[9] This may explain why the current of H_2^+ was the lowest with Al liner in experimental materials.

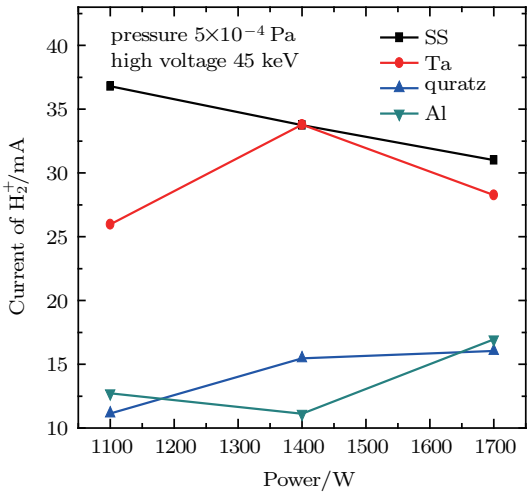


Fig. 2. (color online) H_2^+ current versus rf power for different materials.

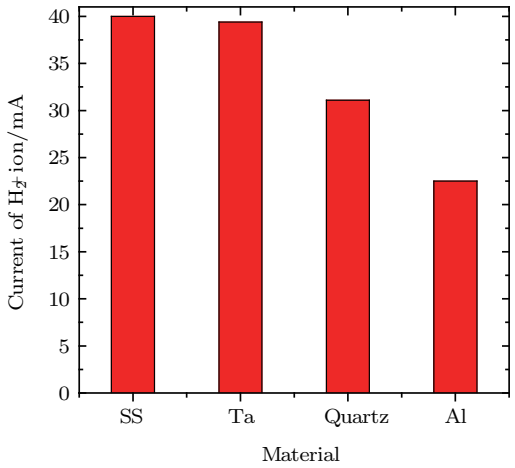


Fig. 3. (color online) Optimized H_2^+ currents varying with category of material.

3.2. Effect of O_2 discharge

It was found in our experiment that after the plasma discharging with O_2 in the chamber, there was an increasing trend for the H_2^+ fraction working with H_2 again. To investigate the effect of O_2 discharge, the fraction of H_2^+ was compared with those in the cases of two kinds of chamber surfaces: native SS surface directly from factory (S1) and SS surface after O_2 discharge (S2). For S2, the O_2 discharge was sustained for 5 hours with power 1400 W and pressure 4×10^{-4} Pa, and the energy of O^+ was several eV.[14] After that, the ion source vessel was pumped continuously for 2 days to clean impurities before discharging with H_2 flow. Hydrogen discharge results with S1 and S2 were compared in Table 2. It is easy to find out that the fraction of H_2^+ increased from 37.5% to 51.2% after O^+ ion bombardments on SS surface under the same operation parameters (1400 W and 7.5×10^{-4} Pa). Even after 20-h hydrogen discharge, the H_2^+ fraction would not decrease according to our experiment.

Table 2. Ion fractions measured with native SS surface and SS surface after O_2 discharge.

SS surface	H^+	H_2^+	H_3^+
S1	58.4%	37.5%	4.1%
S2	41.5%	51.2%	7.3%

3.3. Surface investigations

The reason for the effect of O_2 discharge was not so clear. For analyzing the changes on the chamber wall, several square SS samples each with a dimension of 1×1 cm and thickness of 1.5 mm were fabricated. These pieces were placed on the surface of the discharge chamber to simulate the environment under O^+ or H^+ bombardments, and the pieces were all polished by sand paper to keep the roughness the same prior to treatment. The discharge parameters were shown in Table 3. Then an Agilent 5500 atomic force microscope was used to analyze the morphology and an x-ray photoelectron spectroscope on an AXIS-Ultra instrument from Kratos Analytical was used to analyze the constitutes.

Table 3. Treatment conditions for SS samples.

Sample series	Treat condition
1	untreated
2	O^+discharge for 5 hours
3	H^+ discharge for 20 hours
4	Firstly, O^+ discharge for 5 hours; then H^+ discharge for 20 hours

Figure 4 shows the typical three-dimensional (3D) AFM images, and figure 5 shows the surface roughness R_a measured by AFM. The surface of sample 2 becomes obviously uneven after O^+ discharge as shown in Fig. 4(b). The roughness increased from 55 nm to 73 nm due to O^+ bombardments. It was in accordance with the result from Zhao *et al.*[15] Interestingly, it is also shown in Fig. 5 that the roughness values of SS do not vary obviously after 20-h H_2 discharge by comparing roughness values of samples 3 and 4 with those of samples 1 and 2 separately.

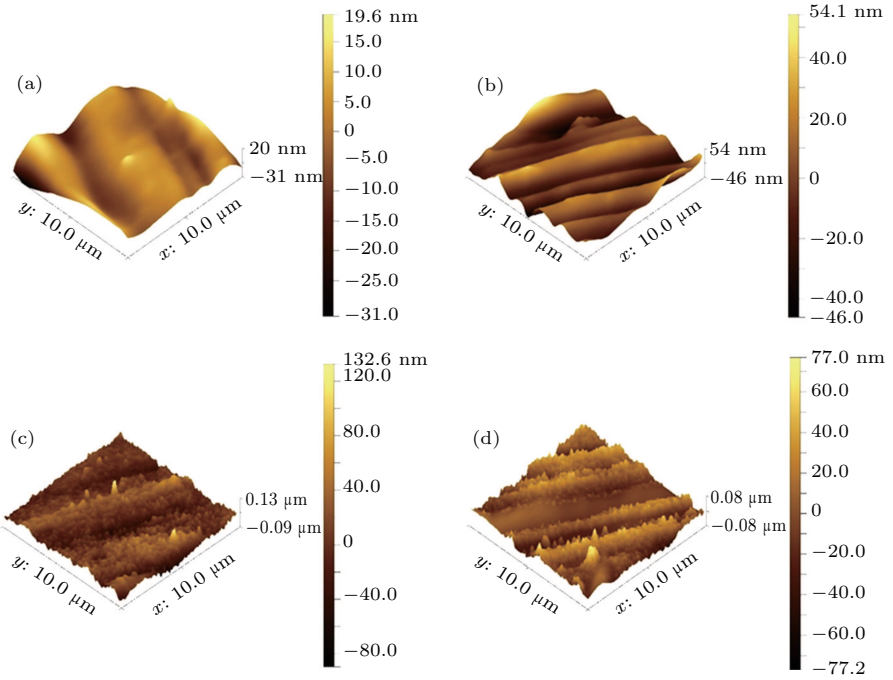


Fig. 4. (color online) AFM 3D images: (a) untreated 1, (b) O_2 discharge, (c) H_2 discharge. (d) first O_2, then H_2 discharge.

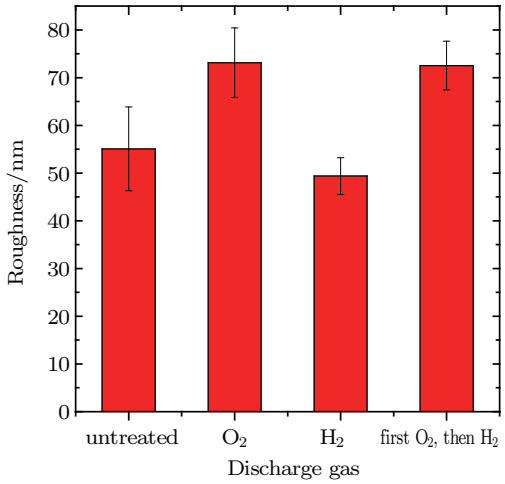


Fig. 5. (color online) Roughness of sample surfaces under different discharge conditions.

Aleksander Drenik *et al.* found the relationship between roughness and the recombination possibility of hydrogen atoms on fine-grain graphite surface,[16] indicating that the recombination coefficient γ increases with the roughness increasing. This can be explained by two facts: firstly, the effective surface for recombination has actually increased due to the increase of roughness; meanwhile, more than one collision between atoms and the surface will happen on an uneven surface compared with on a flat surface. For metal, the recombination coefficient could also increase due to the increase of roughness. So the increasing of roughness caused by O^+ bombardments, which leads to a higher recombination coefficient, may be mainly responsible for the increasing of H_2^+ yield after O_2 discharge.

As an oxide layer could also exist during O_2 discharge, the effect of the oxide layer should be estimated. Actually, unlike the oxide layer of Al, the oxide layer of SS can only exist for a very short time (on the order of second) when exposed to hydrogen plasma because it will be cleaned by hydrogen plasma.[17] Therefore, the influence of oxide should be minimum in hydrogen discharge. In our experiments, the XPS analysis also shows that the relative concentration of O increases after O_2 discharge, but it is recovered to the original value soon after H_2 discharge. So, oxide is indeed not the main reason for the enhancement of H_2^+ ions as it cannot exist in hydrogen plasma.

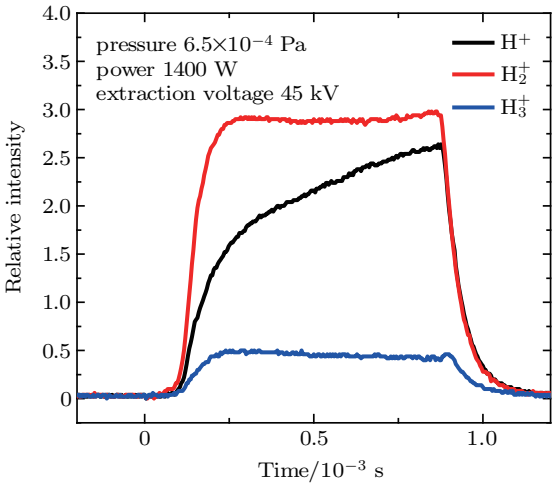


Fig. 6. (color online) Profile of H^+ and H_2^+ and H_3^+.

In conclusion, O^+ discharge with the SS surface is advantageous for the H_2^+ yield. As the effect of the oxide layer

is excluded, it might mainly be caused by the increasing of roughness on SS surface.

After the above study and improvements, a high current H_2^+ ion beam is generated with stainless steel discharge chamber. It can be seen in Fig. 6 that H_2^+ ion has already become the main ion species in the mixing beam. The pure current of H_2^+ ions is improved to 42.3 mA with a fraction of 52.9%.

4. Discussion

A high current H_2^+ ion source is under development at PKU. To obtain more H_2^+ ions, the operation parameters and ion source geometry should be designed thoroughly. In our study, the choosing of wall material is found to have an influence on H_2^+ generation as the recombination possibility varies with material type. Moreover, O_2 plasma discharge can be used to improve the recombination possibility as well as H_2^+ fraction. In the future, an H_2^+ ion source working in CW mode will be designed, and more results will be reported.

References

[1] Calabretta L, Maggiore M, Piazza L A C, Rifuggiato D and Calanna A 2010 in *Proceedings of Cyclotrons* 2010 TUA1CIO01, Lanzhou, China, p. 298

[2] Junquera T 2008 *Proceedings of LINAC08*, TU102, Victoria, BC, Canada, p. 348

[3] Nagler A, Berkovits D, Gertz I, Mardor I, Rodnizki J, Weissman L, Dunkel K, Kremer F, Pekeler M, Piel C and Stein Vom P 2006 in *Proceedings of LINAC* 2006, MOP054, Knoxville, Tennessee, USA, p. 168

[4] Gobin R, Blideanu V, Bogard D, Bourdelle G, Chauvin N, Delferrière O, Girardot P, Jannin J L, Langlois S, Loiseau D, Pottin B, Rousse J Y and Senée F 2010 *Rev. Sci. Instrum.* **81** 02B301

[5] Peng S X, Song Z Z, Yu J X, Ren H T, Zhang M, Yuan Z X, Lu P N, Zhao J, Chen J E, Guo Z Y and Lu Y R 2010 in *Proceedings of ECRIS*10, TUCOCK02, Grenoble, France, p. 102

[6] Ren H T, Peng S X, Xu Y, Zhao J, Chen J, Zhang T, Zhang A L, Guo Z Y and Chen J E 2013 *Sci. China-Phys. Mech. Astron.* **56** 2016

[7] Xu Y, Peng S X, Ren H T, Zhao J, Chen J, Zhang A L, Zhang T, Guo Z Y and Chen J E 2014 *Rev. Sci. Instrum.* **85** 02A943

[8] Waldmann O and Ludewigt B 2011 *Rev. Sci. Instrum.* **82** 113505

[9] Jung B K, Chung K J, Dang J J and Hwang Y S 2012 *Rev. Sci. Instrum.* **83** 02B314

[10] Xu Y, Peng S X, Ren H T, Zhao J, Chen J, Zhang T, Zhang J F, Guo Z Y and Chen J E 2014 in *Proceedings of ECRIS*14, MOOBMH04, Nizhny Novgorod, Russia, p. 20

[11] Mozetič M, Drobnič M and Zalar A 1999 *Appl. Surf. Sci.* **144–145** 399

[12] Grubbs R K and George S M 2006 *J. Vac. Sci. Technol. A* **24** 486

[13] Xu Y, Peng S X, Ren H T, Zhao J, Chen J, Zhang T, Wang Z H, Luo Y T, Guo Z Y and Chen J E 2013 in *Proceedings of IPAC* 2013, MOPFI035, Shanghai, China, p. 363

[14] Melin G, Drentje A G, Girard A and Hitz D 1999 *J. Appl. Phys.* **86** 4772

[15] Zhao Q, Liu Y, Wang C, Wang S, Peng N and Jeynes C 2008 *Med. Eng. Phys.* **30** 341

[16] Drenik A, Vesel A, Kreter A and Mozetič M 2011 *Appl. Surf. Sci.* **257** 5820

[17] Mozetič M, Zalar A and Drobnič M 1999 *Thin Solid Films* **343–344** 101